# Mechanism of densification and crystal perfection of poly(ethylene terephthalate)

**Giovanni Carlo Alfonso, Enrico Pedemonte and Lorenzo Ponzetti**
*Centro di studi Chimico-Fisici di Macromolecole Sintetiche e Naturali, CNR, c/o Istituto di Chimica Industriale, Università di Genova, 16132 Genoa, Italy*
*(Received 22 May 1978; revised 17 July 1978)*

Amorphous poly(ethylene terephthalate) has been isothermally annealed in a wide range of temperatures from $T_g$ to $T_m$. The effects of temperature and time of thermal treatment on density, melting curve and WAXS have been systematically explored. The results showed that densification and crystal perfection take place through a step mechanism involving partial melting and diffusion. The evaluation of the activation energies suggests that diffusion is the rate determining step in the low temperature range.

## INTRODUCTION

Prolonged annealing treatment of amorphous poly(ethylene terephthalate) (PET) produces two endothermal peaks when the polymer is heated in a differential scanning calorimeter.

This behaviour is not peculiar to PET but the presence of multiple endothermal peaks in the melting curve is quite general. Many papers in the last few years collect together results concerning polyethylene[1-3], polypropylene[4-9], polyoxymethylene[10], polystyrene[11-16], poly(vinylidene fluoride)[17], nylons[12,18-24] and other polymers[25-29]; the wider studies were devoted to PET[12,20,21,30-38].

The thermal behaviour exhibited by these polymers is always connected with the previous history of the sample, i.e. thermal and/or mechanical history. It has been attributed either to multiple crystal modifications, to different types of morphology (extended- or folded-chain crystals), to orientation effects or to melt-recrystallization processes.

At present the double peak in PET is explained by the assumption that a recrystallization process takes place during the thermal scanning[32,34,36]. The peak at lower temperature is related to the melting of the crystallites grown at the crystallization conditions and the higher temperature peak derives from melting and recrystallization processes on increasing temperature.

It was shown[34] that only the melting behaviour is strongly affected by the crystallization time, other properties such as density and breadths of X-ray reflections being relatively insensitive. Therefore it was necessary to assume that structural transformations which have little effect on density and X-ray perfection but affect strongly the melting point, take place during annealing. Reasonably these transformations must occur inside the spherulitic structure[34,36].

A process of regularization of the crystals, both inside and on the surfaces, must be assumed since the fold period stays constant or even decreases during isothermal crystallization[39-41]. It will lead to a lower number of crystal defects and to lower values of surface free energies, this involving not only refolding but also chemical reactions between chain segments in the disordered part of the sample[42,43].

Notwithstanding the relevant number of papers available in literature on the annealing of PET, at present it is impossible to utilize results published by different workers for the study, from a kinetic point of view, of the densification and the crystal perfection associated with the secondary crystallization.

The aim of the present work is to collect homogeneous data with different techniques and over a wide range of crystallization conditions in order to give an overall picture of the transformations during thermal treatment. This will enable us to try a kinetic analysis of the phenomena.

## EXPERIMENTAL

### *Material and thermal treatments*

PET was in the form of unoriented pellets, 4 x 5 x 2.5 mm in size, exhibiting no crystallinity on X-ray diagrams and a density value of 1.336 ± 0.001 g/cm$^3$.

Isothermal crystallization was carried out in an oven with forced circulation of air over a range of temperatures ($T_a$) between the glass transition temperature and the equilibrium melting point. Crystallization times ($t_a$) were chosen to cover evenly two or three decades in a logarithmic plot. After appropriate holding times at $T_a$ the pellets were quenched in a water, ice and sodium chloride mixture.

Apparently no degradation process is present up to 240°C; at higher temperatures, for long annealing times, the samples begin to yellow at the surface; in these cases only the inner part of the samples was examined.

### *Density*

Densities were measured at room temperature using a conventional density gradient column[44] filled with a carbon tetrachloride/n-heptane mixture. Care was taken to prepare a linear gradient (about 10 x 10$^{-5}$ g/cm$^3$ mm) over the whole range of interest (1.3300–1.4500 g/cm$^3$).

Samples were degassed for 1 h, wetted with the lighter mixture while in the vacuum line and then transferred in the column, avoiding any contact with air. The position

0032–3861/79/010104–09$02.00

*Table 1* Density data, $\rho$ (g/cm$^3$), for annealed PET samples

| Annealing temperature $T_a$ (°C) | Annealing time, $t_a$ (min) | | | | | | | $B \times 10^3$ | Correlation coefficient $r$ |
|---|---|---|---|---|---|---|---|---|---|
| | 10 | 35 | 100 | 360 | 990 | 3600 | 9900 | | |
| 95 | 1.3373 | 1.3373 | 1.3373 | 1.3381 | 1.3379 | 1.3430 | 1.3581 | – | |
| 110 | 1.3371 | 1.3431 | 1.3635 | 1.3680 | 1.3698 | 1.3705 | 1.3725 | 2.86 | 0.976 |
| 125 | 1.3385 | 1.3700 | 1.3731 | 1.3747 | 1.3755 | 1.3775 | 1.3783 | 2.65 | 0.995 |
| 140 | 1.3382 | 1.3740 | 1.3768 | 1.3777 | 1.3802 | 1.3816 | 1.3825 | 3 41 | 0.985 |
| 155 | | 1.3762 | 1.3780 | 1.3786 | 1.3807 | 1.3825 | | 3.04 | 0.987 |
| 170 | 1.3692 | 1.3804 | 1.3817 | 1.3857 | 1.3880 | 1.3926 | | 6.14 | 0.991 |
| 185 | 1.3725 | 1.3821 | 1.3848 | 1.3895 | 1.3924 | 1.3978 | | 7.79 | 0.997 |
| 200 | 1.3774 | 1.3840 | 1.3871 | 1.3935 | 1.3968 | 1.4037 | | 9.81 | 0.996 |
| 215 | 1.3789 | 1.3884 | 1.3936 | 1.4010 | 1.4064 | 1.4155 | | 13.37 | 0.998 |
| 230 | 1.3876 | 1.3926 | 1.4015 | 1.4108 | 1.4162 | | | 15.09 | 0 994 |
| 245 | 1.3950 ° | 1.4000 | 1.4077 | 1.4152 | | | | 14.97 | 0.999 |
| 255 | 1.3937 | 1.4021 | 1.4103 | 1.4170* | | | | 16.95 | 0.999 |

° $t_a$ = 15 min *, $t_a$ = 240 min

of the pellets was compared with those of calibrated glass standards after the forces equilibrium was reached, i.e. about 3 h.

Each result reported in *Table 1* is the average of five measurements on different pellets with the same thermal history. Samples with density values deviating more than $3 \times 10^{-4}$ g/cm$^3$ from the average were neither considered for the average itself nor for the other measurements.

Possible errors deriving from interfacial tensions, when analysed taking into account the shape of the pellets and the density gradient along the column[45], were estimated less than $2 \times 10^{-4}$ g/cm$^3$.

*Thermal analysis*

A Perkin–Elmer differential scanning calorimeter DSC-1B was used under inert atmosphere and with heating rates between 2.0° and 64°C/min. Generally the melting curves were obtained at 32°C/min; the other temperature regimes were used only to analyse the effect of the heating rate on the melting behaviour of the polymer.

The instrument was calibrated, both in temperature and melting enthalpy, with standard samples of indium and tin.

To avoid an uneven thermal conduction through the samples, which causes different amounts of broadening and shifting of the peak positions, the aluminium pans were always filled with the same quantity of polymer (15 ± 1 mg), in the form of small grains cut with razor blades from the annealed pellets.

The two fusion endotherms were as indicated according to Fakirow *et al.*[41]: $T'_m$ and $T''_m$ correspond to the temperature positions of the first and of the second peak, respectively. The melting temperatures were always corrected for the effect of the heating rate on the instrumental time lag.

The melting enthalpies were calculated from the area between the curve and the baseline; the peaks partly superimposed were resolved into their components curves as in ref 41.

*X-ray diffraction*

A General Electric XRD-3 automatic diffractometer was used, employing a Ni-filtered CuKα radiation detected by a scintillation counter. Diffractograms were recorded by continuous scanning at a rate of 2°/min over the range of $2\theta$ from 8° to 38°.

The thickness of the annealed pellets were reduced to 0.5 mm by slow multidirectional abrasion on 500 mesh abrasive powder while immersed in water to avoid any heating effect.

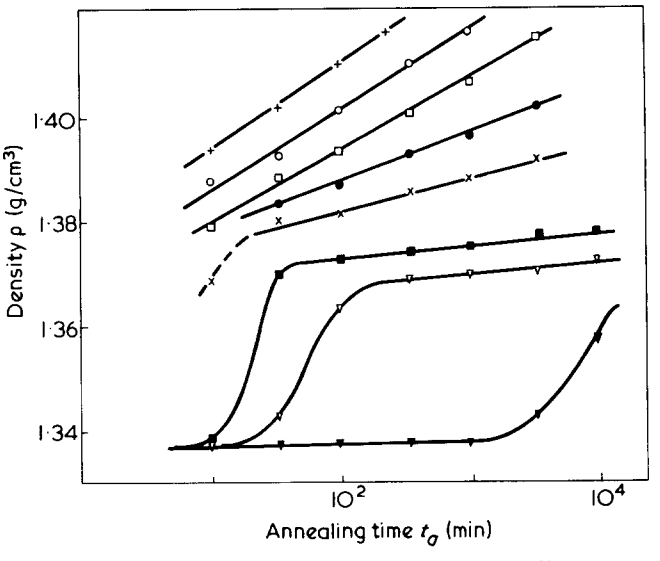


*Figure 1* Dependence of density on annealing time at different annealing temperatures. ▼, 95°C; ▽, 110°C; ■, 125°C; x, 179°C; ●, 200°C; □, 215°C; ○, 230°C; +, 255°C

The apparent crystallite dimensions $L_{100}$, perpendicular to (100) plane, were estimated from the uncorrected breadth, $\beta_0$, at half-maximum intensity of the 100 reflections using the conventional equation[46]:

$$L_{100} = \frac{K\lambda}{\beta_0 \cos\theta} \quad (1)$$

assuming $K$ = 1.0.

## RESULTS

*Density*

Density data of all annealed samples are reported in *Table 1*; *Figure 1* shows the trends of $\rho$ *versus* $t_a$ for several temperatures.

In the low temperature range primary crystallization is slow enough to be detectable with our technique. The development of crystallinity can be followed with sufficient accuracy up to $T_a$ = 125°C; at higher temperatures primary crystallization goes to completion in a very short time and non-isothermal processes affect the kinetics and lead to lower values of density[47].

Densification at long times is linearly dependent on

$\log t_a$; similar results were previously reported by various authors for some different polymers[2,48–51].

The experimental results of *Figure 1* fit the general equation:

$$\rho(t_a) = \rho_0 + B\log(t_a/t_0) \qquad (2)$$

where $\rho_0$ is the value of the density at $t_0$, the starting point of the secondary crystallization, and $B$ is a parameter related to the rate of the process.

Our calculated values of $B$ show a definite increase with $T_a$, as reported in *Table 1* and shown in *Figure 2*. Both the slopes $B$, and the correlation coefficient, $r$, were calculated using regression analysis on a Texas Instruments TI-59 pocket computer.

Holdsworth and Turner-Jones[34] did not find any appreciable change in density with the annealing time, probably due to their particular annealing technique. On the other hand the trend shown in *Figure 2* is qualitatively in agreement with other data available in the literature[52–54].

*Thermal analysis*

It has been already demonstrated that the melting curves exhibit one or two peaks depending on the annealing treatment[12,20,21,30–38]. In our experimental conditions two peaks

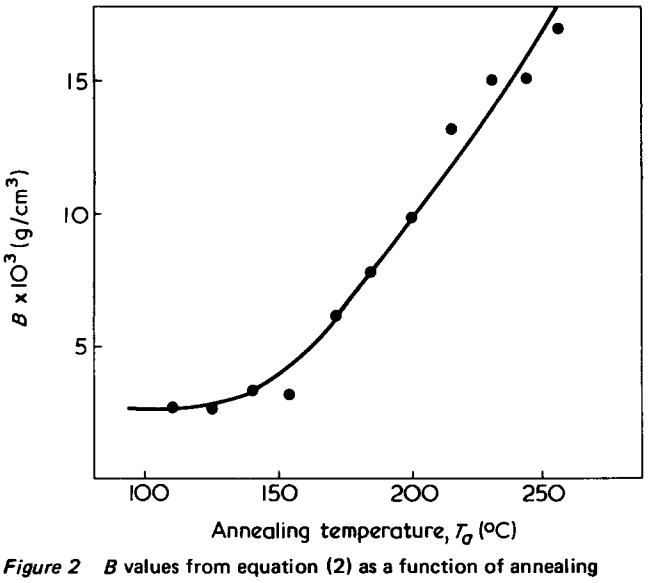


*Figure 2* $B$ values from equation (2) as a function of annealing temperature

are present up to $T_a$ = 200°C for all annealing times investigated; between 200° and 230°C only one peak can be observed for the longer annealing times and finally, above $T_a$ = 230°C, the second endotherm is never present.

When two peaks appear, $T_m''$ is constant (about 253°C) whatever are $T_a$ or $t_a$; $T_m'$ increases both with annealing time and temperature and it is usually found about 10°–30°C above $T_a$. According to Roberts[31] and Holdsworth *et al.*[34] the first endothermic peak of the curve must be related to the melting of the crystals formed at $T_a$ which can slightly increase in perfection during heating in d.s.c. The second peak is attributed to the final melting of the material recrystallized above $T_m'$ during the scan. If $T_m'$ is sufficiently high the recrystallization process can no longer take place owing to the relatively small undercooling and hence only one peak will appear.

With the aim of giving additional experimental support to this interpretation, particular thermal histories were applied to the original amorphous pellets; these involve two subsequent annealing treatments at $T_{a1}$ and $T_{a2}$ separated by a quenching. The results can be summarized as follows:

(1) Samples annealed at $T_{a1}$ = 170°C for 6 h and then at $T_{a2}$ = 200°C for 6 h. Both final density (1.3935 g/cm$^3$) and fusion curve (double peak and $T_m'$ = 227°C) are identical to those exhibited by samples annealed only once at 200°C for 6 h.

(2) Samples annealed at $T_{a1}$ = 200°C for 6 h and then at 170°C for 35, 100, 360 and 990 min. The final density is still 1.3935 independent of the duration of the second annealing ($t_{a2}$). The d.s.c curve is still superposable on that of samples treated at 200°C for $t_{a2}$ up to 360 min. For $t_{a2}$ = 990 min, there emerges a broad extra peak, centred about 195°C. Its area is smaller than that of a sample annealed only once at 170°C for the same time, the position being still the same.

The application of various heating regimes, from 2° to 64°C/min, to specimens annealed at different temperatures and times lead to results similar to those reported in literature[32,42,43] i.e. a superheating effect is evident for the low temperature peak $T_m'$ whose associated melting enthalpy decreases with heating rate.

These observations show that the low temperature endotherms are related to the melting of crystals with size and perfection characteristics related to the crystallization conditions (temperatures and times).

*Table 2* summarizes the experimental values of $T_m'$ as functions of $T_a$ and $t_a$ and in *Figure 3* the trends at some annealing temperatures are drawn.

*Table 2* Melting temperatures, $T_m'$ (°C), for annealed PET samples

| Annealing temperatures $T_a$ (°C) | Annealing times, $t_a$ (min) | | | | | | | $D$ | Correlation coefficient $r$ |
|---|---|---|---|---|---|---|---|---|---|
| | 10 | 35 | 100 | 360 | 990 | 3600 | 9900 | | |
| 110 | | | (109) | 117 | 121 | 124 | 129 | 7.95 | 0.990 |
| 125 | | 129 | 131 | 136 | 139 | 143 | 147 | 7.45 | 0.997 |
| 140 | | 144 | 151 | 155 | 157 | 165 | 167 | 9.15 | 0.987 |
| 155 | | 156 | 159 | 163 | 168 | 174 | | 9.35 | 0.995 |
| 170 | | 177 | 184 | 189 | 195 | 207 | | 14.15 | 0.987 |
| 185 | (147) | 196 | 204 | 213 | 221 | 226 | | 15.30 | 0.993 |
| 200 | (167) | 208 | 217 | 227 | 231 | 241 | | 15.95 | 0.995 |
| 215 | (173) | 224 | 232 | 238 | 244 | 250 | | 12.70 | 0.996 |
| 230 | (231) | 237 | 244 | 252 | 255 | 258 | | 11.10 | 0.985 |
| 245 | (242)° | 259 | 264 | 267 | 271 | 274 | | 7.35 | 0.992 |
| 255 | 261 | 265 | 268 | 270* | | | | 5.75 | 0.983 |

° $t_a$ = 15 min *, $t_a$ = 240 min

The data in brackets lying below or very near to $T_a$, are not considered as significant owing to the non-isothermal processes previously discussed. In the samples annealed for short times there occur crystals formed over a wide range of temperatures which had not enough time to reorganize themselves in a more regular structure; hence they will have a wide range of perfection and thickness.

In the whole range of $T_a$ the dependence of $T_m'$ on $t_a$ follows the logarithmic law:

$$T_m'(t_a) = T_0 + D\log(t_a/t_0) \qquad (3)$$

where $T_0$ is the melting temperature of crystals at the beginning of the secondary crystallization, $t_0$, and $D$ is a temperature dependent parameter.

Equation (3) is in agreement with the results of Roberts[31] and it can be demonstrated that it fits the data reported for PET by some authors (see *Table 3*). A similar relationship was observed occasionally for polyolefins[2,6,55] and nylons[56].

Our values of $D$ are plotted against $T_a$ in *Figure 4* together with the data deduced from *Table 3*. The misfit of some of them can be attributed both to differences in molecular weights and in the annealing procedure and to the effect of heating rate on $T_m'$ [43]

*X-ray diffraction*

The apparent minimum crystallite dimensions $L_{100}$ calculated from equation (1) are shown in *Figure 5* as a function of annealing time for three different temperatures.

Despite of the rough estimate of $\beta_0$, it is evident that $L_{100}$ is larger the higher is the annealing temperature. However the main information that one can draw from this figure is that $L_{100}$ also depends linearly on log $t_a$; besides this, the rate of increase has a maximum around 185°C.

Data reported in literature[34,39] indicate a small variation of $\beta_0$ on time. This fits with our results since those observations refer to annealing temperatures higher than 220°C.

$\beta_0$ is related not only to crystal size but also to defects and lattice distortions. This implies that our values of $L_{100}$ are undervalued and that the apparent variations could be partly or entirely due to segregation of defects from the crystalline regions.

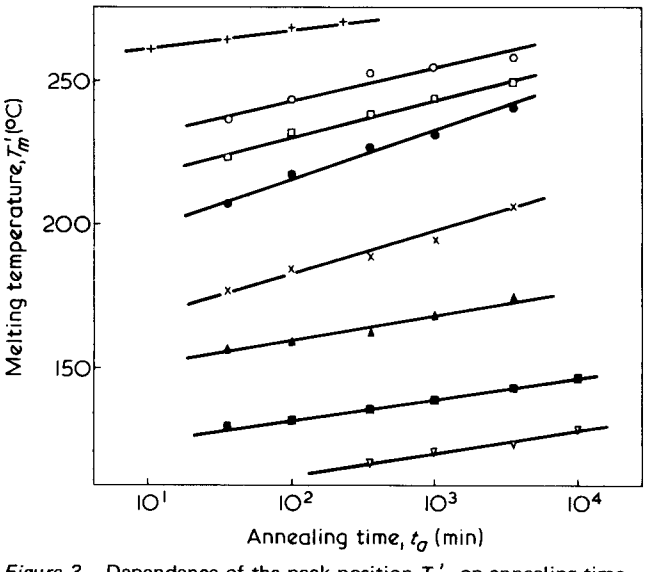


*Figure 3* Dependence of the peak position $T_m'$ on annealing time at different annealing temperatures. ▲, 155°C; other symbols as in *Figure 1* (Heating rate 32° C/min)

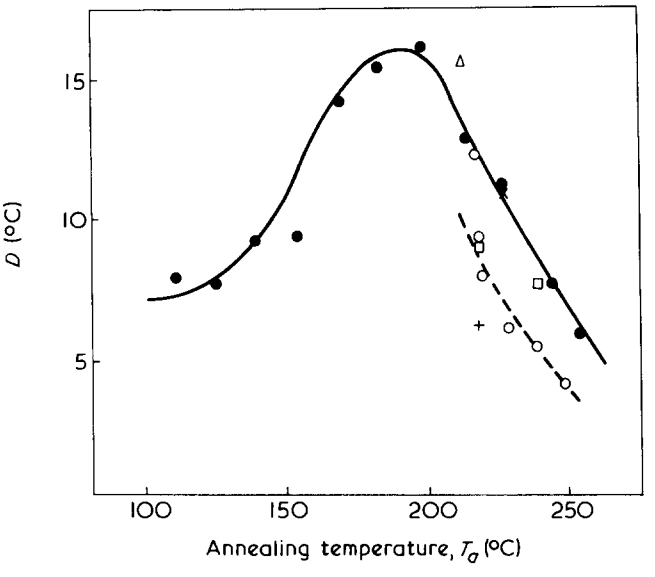


*Figure 4* D values from equation (3) as a function of annealing temperatures: ●, this work; ○, from ref 31; +, from ref 20; x, from ref 21; △, from ref 33; □, from ref 34

*Table 3* Rate of shifting of $T_m'$ from literature data

| $T_a$ (°C) | D | r | Thermal history | Heating rate | Reference |
|---|---|---|---|---|---|
| 215 | 15.6 | 0.978 | Crystallized from the melt at 140° C for six half-times of crystallization and then annealed | 20° C/min | Nealy *et al.*[33] |
| 220 | 8.9 | 0.997 | Crystallized from the glassy state by heating in d.s.c. up to $T_a$ | 16° C/min | Holdsworth *et al.*[34] |
| 240 | 7.4 | 1.000 | at 16° C/min | 16° C/min | Roberts[31] |
| 220 | 12.0 | 0.983 | Crystallized from the melt | | |
| 220 | 7.8 | 1.000 | Cooled from the melt at 64° C/min, crystallized at 100° C and | 16° C/min | Roberts[31] |
| 230 | 5.8 | 1.000 | reheated up to $T_a$ at 64° C/min. (Short annealing times) | | |
| 240 | 5.3 | 0.980 | | | |
| 250 | 3.9 | 1.000 | | | |
| 220 | 9.0 | – | Cooled from the melt at 64° C/min, crystallized at 100° C and reheated up to $T_a$ at 64° C/min (Long annealing times) | 16° C/min | Roberts[31] |
| 220 | 6.2 | 0.987 | Crystallized from the glassy state for 30 min at 110° C and annealed at 220° C | 10–20° C/min | Bell *et al.*[20] |
| 230 | 11 | – | Crystallized from the glassy state at 110° C for 30 min and then annealed | 10° C/min | Sweet *et al.*[21] |

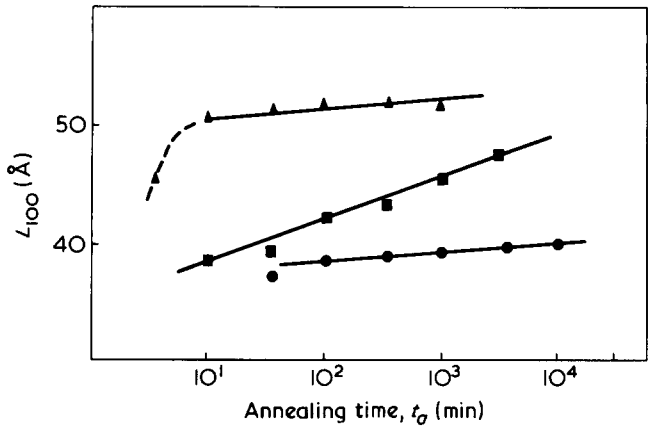


*Figure 5* Apparent crystallite dimensions as a function of annealing time for three different temperatures. ●, 140°C; ■, 185°C; ▲, 230°C

On increasing annealing time an increase of X-ray crystallinity was always observed; the extent of this increase being dependent on temperature qualitatively in agreement with density data.

## DISCUSSION

Our data show that the increase of density during secondary crystallization is considerable, particularly at high temperatures. Densification in isothermal conditions can be envisaged as a slow transformation to which, in principle, several phenomena can contribute: lamellar thickening, reorganization of amorphous regions, rejection of defects from crystals, and crystallization of amorphous chain segments.

It is already widely demonstrated[39–41,57] that long time annealing of PET does not involve any increase in long spacing; on the contrary, undrawn material slightly decreases its small angle periodicity.

Changes in amorphous density during the secondary crystallization were observed in poly(tetramethylene oxide)[50]. Fisher *et al.*[41,57] have found that the effective amorphous density of drawn and undrawn PET depends on temperature. However, the observed variations were very small so that this phenomenon seems to contribute only to a negligible amount of the overall densification.

According to a mosaic block model[58] of the crystallites in which the crystalline regions are considered as built up of small and regular domains separated from each other by layers of amorphous packed molecules (*Figure 6*), one can try to distinguish if the densification is due to the growth of the mosaic blocks or to the formation of new ones inside the amorphous phase in which crystallites are embedded.

Some general information about these contributions can be obtained by considering the sharpening of the WAXS profile on time at constant temperature. If we assume (as in *Figure 5*) that the breadth of peak derives only from the crystal size, it is possible to calculate the increase of density corresponding to the mosaic block growth. Only at 185°C, where the largest variation of $L_{100}$ is observed, is the related increase of density approximately equal to the experimental value. At 140° and 230°C calculations lead to density variation at least one order of magnitude lower than the experimental findings. Due to the assumptions, the calculated increase of density is certainly overestimated and therefore we can conclude that a considerable contribution to the densification is given by the formation of new blocks in the amorphous phase.

Discussion is still open about the contribution of rejection of defects from crystalline regions. According to Geil[59] the perfection of a crystal is determined also by its rate of formation during primary crystallization; hence at temperatures near $T_g$ and $T_m^0$ blocks with a lower number of defects than those formed at intermediate temperatures can be expected. For PET the maximum crystallization rate was observed in the range of 180°C[47]; this can account for our experimental findings related to the variations of the half-breadth of the diffraction peaks with time at different temperatures.

The model drawn in *Figure 6* explains not only the densification discussed above but also the remarkable increase of $T_m'$ on time shown in *Figure 3*.

The actual melting point of a polymer crystal was proved to be related to its shape and surface energies through the relationship[60]:

$$T_m' = T_m^0 \left(1 - \frac{2\sigma_e}{\Delta H^0 \rho_c l} - \frac{4\sigma}{\Delta H^0 \rho_c a} - \frac{c_d \bar{\epsilon}_d}{\Delta H^0 \rho_c}\right) \qquad (4)$$

where $\sigma_e$ and $\sigma$ are the surface free energies respectively of the folding and lateral surfaces of a prismatic crystal with thickness $l$ and cross section $a^2$; $c_d$ is the concentration of all kinds of defects in the crystals and $\bar{\epsilon}_d$ is the associated mean value of excess free energy. Finally $\Delta H^0$ is the melting enthalpy of an ideal crystal ($\Delta H^0$ = 24.3 kJ/mol)[61] and $\rho_c$ is the density of the crystal phase (1.457 g/cm$^3$)[61]. $T_m^0$, the equilibrium melting point was assumed to be 284°C[62].

The low melting temperature at the beginning of the secondary crystallization is direct evidence that the crystals are not in the state of maximum stability. We have to discuss how the system reaches a lower free energy level.

In the frame of the assumed model since $l$ and $a$ do not undergo substantial changes with time, the increase of $T_m'$ must be attributed to processes that lead to lower values of the surface energies and to a lower concentration of defects of smaller energy content.

If in the right-hand side of equation (4) all the parameters but $\sigma_e$ are assumed to be constant with time, it is possible to evaluate its variation from the experimental values of $T_m'$. Calculations of the folded surface free energy lead to 50 erg/cm$^2$ at high temperatures and values up to 300 erg/cm$^2$ are obtained on decreasing annealing temperature; the changes of $\sigma_e$ over two decades of the secondary crystallization are in the range 20–50 erg/cm$^2$ depending on tempera-

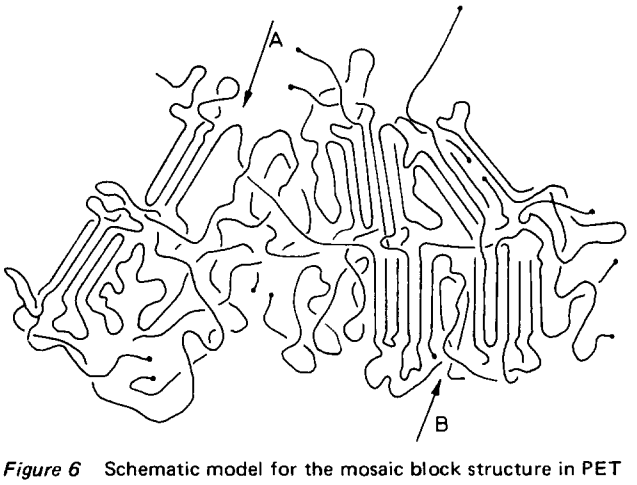


*Figure 6* Schematic model for the mosaic block structure in PET

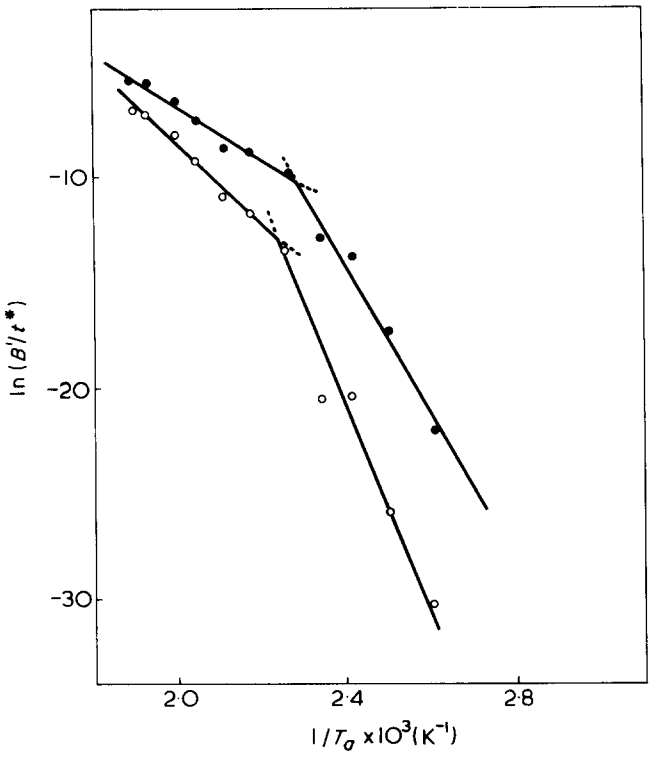


*Figure 7* Plot of experimental values according to equation (8). ○, $\rho^* = 1.3900$ g/cm$^3$; ●, $\rho^* = 1.3800$ g/cm$^3$

ture. At high temperatures the relative variation of $\sigma_e$ is about 50%; this figure seems too high and therefore also the rejection of defects and the regularization of the lateral surfaces must be considered.

Summarizing, the densification seems to involve the crystallization of the amorphous chain segments in additional blocks of the mosaic; the increase of the melting temperature must be related to molecular movements that take place inside the crystals: both into the blocks and on their non-ordered boundaries. Therefore the variations of $\rho$ and $T_m'$ do not need to be strictly related since they involve movements of chain segments which are unevenly hindered.

The increase in the densification rates with annealing temperatures (*Figure 2*) is directly related to some molecular mechanism whose rate-determining step is not the formation of nuclei of critical sizes. In the latter case the driving force increases on decreasing temperature[60] and a negative temperature coefficient of the densification rate would be foreseen.

In order to get additional information about the mechanism of the phenomenon, one has to look at the rate constants and to estimate the activation energy.

From equation (2) it follows that the rate of density variation, $v_\rho = d\rho/dt$, is related to our experimental data through:

$$v_\rho = \frac{d\rho}{dt} = \frac{1}{t}\frac{d\rho}{d\ln t} = \frac{B}{2.303t} = \frac{B'}{t} \qquad (5)$$

which is substantially the same equation obtained by Peterlin for the isothermal thickening of polyethylene[63,64] and applied by Karr *et al.* to polyoxymethylene[70].

On the other hand the rate equation can also be written as:

$$v_\rho = K_\rho F(\rho) \qquad (6)$$

where $K_\rho$ is the temperature dependent rate constant and $F(\rho)$ is an undetermined function of the density.

We will assume that $F(\rho)$ depends merely on the level of macromolecular organization reached both in crystalline and amorphous phases; this would imply that the system can be characterized by the value of density alone, independently of the concentration of defects in the crystals and of the pre sence of some local order in the amorphous regions. Hence we assume that, at constant temperature, systems exhibiting the same value of density do evolve with the same rate whatever their previous thermal history.

It follows that, for every arbitrarily chosen value of density $\rho^*$, equation (6) reduces to:

$$v_\rho = K_\rho F(\rho^*) = K_\rho' = K_{0\rho} \exp \frac{-E_{a\rho}}{RT} \qquad (7)$$

where $K_{0\rho}$ is a parameter slightly dependent on temperature and $E_{a\rho}$ is the activation free energy of the densification process at $\rho^*$.

From equations (5) and (7) it can be obtained:

$$\ln\left(\frac{B'}{t^*}\right) = \ln K_{0\rho} - \frac{E_{a\rho}}{RT} \qquad (8)$$

where $t^*$ is the temperature dependent time necessary to reach the density $\rho^*$ in the course of the secondary crystallization. This time can be directly read out from the $\rho$ *versus* log $t$ diagram or must be evaluated through the extrapolation of the linear part of the plot.

The activation free energy can be evaluated from *Figure 7* where data are plotted according to equation (8) for two values of $\rho^*$.

The fitting of each set of data needs two straight lines, crossing each other around 170°C. It is well known that a change in activation energy with temperature indicates a shift in the controlling mechanism of the process; in particular a drop in $E_a$ value indicates that the controlling mechanism has shifted from one of a succession of elementary steps to another in the series. On this basis our plot can be interpreted as deriving from a process consisting of three consecutive steps:

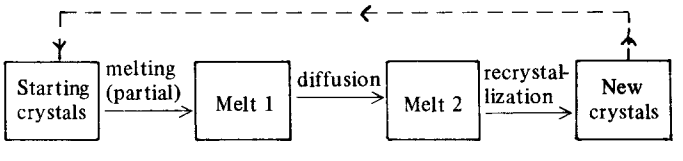


In our understanding 'partial melting' means the removal of local constraints on the amorphous chain segments due to the trapping of segments into the ordered blocks (*Figure 6*); consequently the non-crystalline segment sequences will gain enough mobility to reorganize themselves inside the amorphous regions (chain A) or at the boundaries of the blocks (chain B).

In this succession of steps the recrystallization, that would involve secondary nucleation on the preexisting crystalline substrates, is never the rate-determining step since a positive temperature coefficient is always observed.

At low temperatures the evaluated activation energy is about 335 kJ/mol; this figure for $E_{a\rho}$ is comparable with the value reported by Collier and Baer[65] for the diffusion process of PET crystallizing from the glassy state. Consequently up

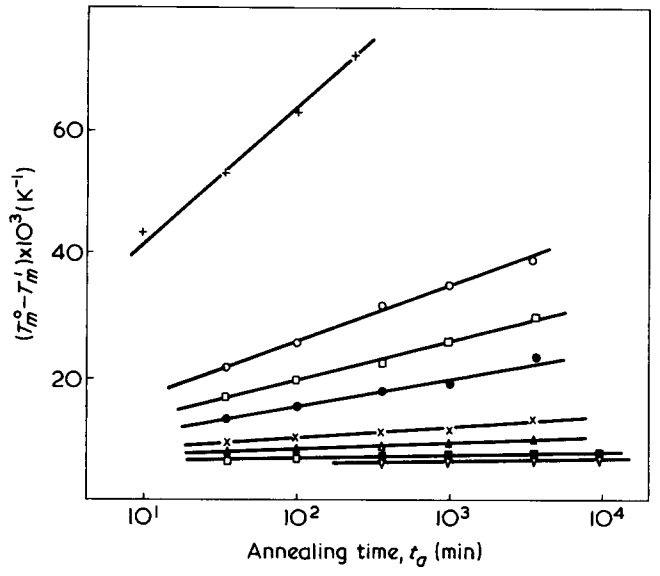


*Figure 8* Relationship between $(T_m^0 - T_m')^{-1}$ and annealing time and temperature. Symbols as in *Figure 3*

to about 170°C the diffusion of amorphous chain segments appears to be the controlling step.

At temperatures higher than 170°C, $E_{a\rho}$ is about 125 kJ/mol. By applying to our results the approach developed by Sanchez *et al.*[66,67] for the isothermal crystal thickening, ascribing to the cooperative melting of a minimum number $\upsilon$ of monomeric units the role of rate determining step, it follows from $E_{a\rho} = \upsilon\Delta H_m^0$ that at high temperatures the densification is controlled by the fusion of about 5 monomeric units. This figure is slightly smaller than the calculated number of units present in a single traverse of a crystalline block[39,40,43,61,68,69]. As a matter of fact the crystals are not ideal and therefore, in order to remove a traverse, it seems reasonable to supply an amount of energy smaller than that necessary for melting the number of monomeric units corresponding to the value of the long period.

It is noteworthy that both the activation energies increase with $\rho^*$. This again is consistent with the proposed mechanism since with the progress of the densification the remaining amorphous chain segments are expected to be more and more hindered by crystalline blocks of increased perfection.

Finally we observe that breaks in the plot of *Figure 7* are located around the temperature at which primary crystallization rate has a maximum owing to the diffusion to nucleation transition of the rate-determining step.

By analogy with the treatment of density data, the increase of the melting temperature with time can be handled to give the activation energy and information about the mechanism of crystal perfection.

Usually equation (4) is applied taking into account only the contribution to the free energy of the folding surfaces. On this assumption it is possible to correlate the variation of $T_m'$ with changes of blocks thickness $l$ and surface free energy $\sigma_e$:

$$v_T = \frac{dl(\sigma_e)^{-1}}{dt} = \frac{dl(\sigma_e)^{-1}}{d\log t}\frac{1}{2.3t}$$

$$= \frac{2T_m^0}{\Delta H^0\rho_c}\frac{1}{2.3t}\frac{d(T_m^0 - T_m')^{-1}}{d\log t} = A\frac{C}{t} \qquad (9)$$

where $A = 2T_m^0/2.3\Delta H^0\rho_c$ and $C$ is the slope of the $(T_m^0 - T_m')^{-1}$ *versus* log t plot (see *Figure 8*).

The rate of change of the two characteristics of the macroconformation of the polymeric chain $l$ and $\sigma_e$, will presumably be proportional to some function of the macroconformation itself:

$$v_T = K_T G(l/\sigma_e) \qquad (10)$$

where $K_T$ is the temperature dependent rate constant.

We assume that, as $F(\rho)$ in equation (6), $G(l/\sigma_e)$ depends only on the actual value of the ratio $l/\sigma_e$ and hence on the actual melting temperature of the crystals: crystals characterized by the same value of $T_m'$ exhibit the same rate of perfection. In fact thick crystals should have a surface energy higher than thin ones in order to melt at the same temperature.

Also for the crystal perfection we can introduce the activation energy of the process $E_{aT}$ for an arbitrarily chosen value of the melting temperature of the crystals $T_m^*$ by writing:

$$v_T = K_T G\left(\frac{l}{\sigma_e}\right)^* = K_T^* = K_{0T}\exp\left(-\frac{E_{aT}}{RT}\right) \qquad (11)$$

where $K_{0T}$ is a parameter slightly dependent on temperature.

From equations (9) and (11) it follows that:

$$\ln\left(\frac{C}{t^*}\right) = \ln\left(\frac{K_{0T}}{A}\right) - \frac{E_{aT}}{RT} \qquad (12)$$

where $t^*$ is the temperature dependent time necessary to obtain crystals with a melting temperature $T_m^*$ in the course of the secondary crystallization.

Formally this equation does not change if rejection of defects and reorganization of the lateral surfaces of the crystal blocks are considered besides the contribution of the folding surfaces, since all processes are dependent on the same mechanisms.

Values of $C$ and $t^*$ can be obtained from *Figure 8*; these data are plotted in *Figure 9* according to equation (12) for $t^*$ values corresponding to crystals melting at $T^*$ equal to 184° and 234°C.

Also in this case each set of data can be fitted by two straight lines from which the activation energies reported in *Table 4* can be obtained. Again, the crossover occurs at about 180°C where the maximum in *Figure 4* is observed.

These results can be explained if the modification of the macrostructure leading to the increase of the melting temperature are controlled by a step mechanism as previously discussed for densification. In this case, however, the activation energies are much higher. Indeed the amorphous chain segments involved in crystal perfection are located in the crystallites, between the mosaic blocks and at the folding surfaces; tie molecules and tight folds must reach a noticeable mobility in order to overcome the strong constraints due to local topology.

From this picture it follows that the diffusion is strongly hindered and that a large amount of energy must be applied to the system. On the other hand the reorganization of crystals does not require the complete melting of the whole blocks but certainly a liquidlike mobility must be reached cooperatively by a relevant number of monomeric units. The densification process has a large contribution in the

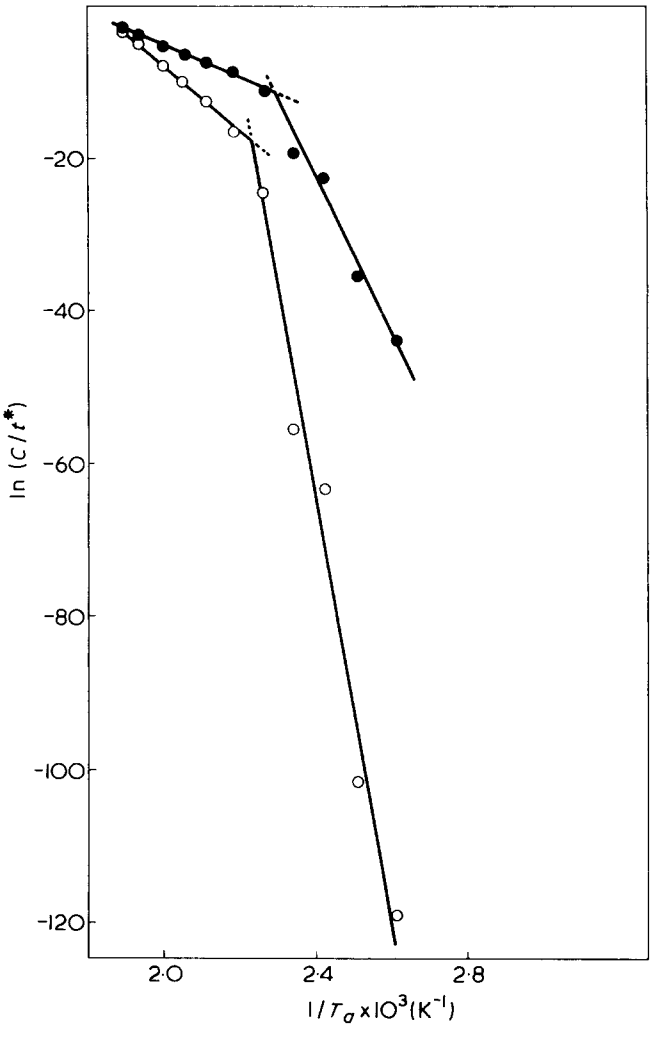


*Figure 9* Plot of experimental values according to equation (12). ○, $T^* = 234°C$; ●, $T^* = 184°C$

formation of new blocks and, as discussed before, can be accounted for by the detachment of a single traverse from the already existing blocks. Detachment of only one stem may be not sufficient to increase the crystal perfection. Therefore the activation energy corresponding to the cooperative melting of several traverses may be required. Our data indicate that two or three traverses must simultaneously reach a liquid-like mobility.

The calculated activation energies increase noticeably with $T^*$; this fact can be accounted for by both the thickening and the rejection of defects which take place into the crystallites during a secondary crystallization and by the more and more reduced mobility of the disordered regions involved in the diffusion process.

Very high value of $E_{aT}$ are not surprising; indeed activation energies of the same order of magnitude have been published recently for the isothermal lamellar thickening of polyoxymethylene[70].

We underline that another possible contribution to crystal perfection may derive from a chemical reorganization process involving reactions on the fold surfaces as suggested by Wunderlich *et al.*[42,43]. For the rupture of the weaker bonds in PET activation energies of about 300–400 kJ/mol are reported[71]; taking into account that the simultaneous breakage of two chains must occur, high activation energies are partly accounted for.

*Table 4* $E_{aT}$ values (kJ/mol) from *Figure 9*

| | $T^* = 184°C$ | $T^* = 234°C$ |
|---|---|---|
| Low temperature range | 775 | 2090 |
| High temperature range | 175 | 350 |

## CONCLUSIONS

A linear increase of density, melting temperature (corresponding to the first peak) and half-breadth of the (100) reflection with the logarithm of annealing time was observed over all range of temperatures from $T_g$ to $T_m^0$; our results are in agreement with the findings of several authors[20,21,31,33,34,41] concerning single techniques and a limited range of annealing conditions.

These results show that the polymer is able to form crystals with a very wide range of perfection depending on crystallization time and temperature. Our experiments also confirm definitively the interpretation of the two peaks in the d.s.c. curves suggested by Holdsworth[34]: i.e. the defective crystallites formed at the annealing temperatures melt and recrystallize during the scanning. It follows that the evaluation of the melting enthalpies from the melting curves is doubtful.

A mosaic block structure for the bulk polymer and a multiple step mechanism for both densification and crystal perfection is suggested. In both processes the step which starts the transformation is the melting of part of the crystals. Densification needs the detachment of one traverse from the blocks, which enables the amorphous polymer segment to move and to build up new blocks together with other amorphous chain segments. Crystal perfection requires the melting of two or three traverses in order to allow their reorganization into blocks with a lower concentration of defects and more regular folding surfaces.

The diffusion of the polymer segments takes place inside the amorphous regions between crystallites in the first case; the second one occurs mainly in the poorly ordered boundaries of the blocks. Consequently, the activation energy for the crystal perfection is higher than that for the densification.

Finally it has been deduced that diffusion is the rate-determining step for both processes at low temperatures while partial melting controls the kinetics above 180°C.

## REFERENCES

1 Prime, R. B., Wunderlich, B. and Melillo, L. *J. Polym. Sci. (A-2)* 1969, **7**, 2091
2 Okamoto, H. *J. Polym. Sci. (A-2)* 1970, **8**, 311
3 Harrison, I. R. *J. Polym. Sci., Polym. Phys. Edn* 1973, **11**, 991
4 Pae, K. D. and Sauer, J. A. *J. Appl. Polym. Sci.* 1968, **12**, 1901
5 Sauer, J. A. and Poe, K. D. *J. Appl. Polym. Sci.* 1968, **12**, 1921
6 Kamide, K. and Yamaguchi, K. *Makromol. Chem.* 1972, **162**, 205
7 Kamide, K. and Yamaguchi, K. *Makromol. Chem.* 1972, **162**, 219
8 Fichera, A. and Zanetti, R. *Makromol. Chem.* 1975, **176**, 1885
9 Samuels, R. J. *J. Polym. Sci. (Polym. Phys. Edn)* 1975, **13**, 1417
10 Jaffe, M. and Wunderlich, B. *Kolloid, Z.* 1967, **216**, 203
11 Boon, J., Challa, G. and van Krevelen, D. W. *J. Polym. Sci. (A-2)* 1968, **6**, 1835
12 Bell, J. P. and Dumbleton, J. H. *J. Polym. Sci. (A-2)* 1969, **7**, 1033
13 Pelzbauer, Z. and Manley, R. St. J. *J. Polym. Sci. (A-2)* 1970, **8**, 649
14 Lemstra, P. J., Kooistra, T. and Challa, G. *J. Polym. Sci. (A-2)* 1972, **10**, 823

15 Pelzbauer, Z. and Manley, R. St J. *J. Macromol. Sci. (Phys.)* 1973, **7**, 345
16 Lemstra, P. J., Schouten, A. J. and Challa, G. *J. Polym. Sci. (Polym. Phys. Edn)* 1974, **12**, 1565
17 Nakagawa, K. and Ishida, Y. *J. Polym. Sci. (Polym. Phys. Edn)* 1973, **11**, 2153
18 Hybart, F. J. and Platt, D. J. *J. Appl. Polym. Sci.* 1967, **11**, 1449
19 Bell, J. P., Slade, P. E. and Dumbleton, J. H. *J. Polym. Sci. (A-2)* 1968, **6**, 1773
20 Bell, J. P. and Murayama, T. *J. Polym. Sci. (A-2)* 1969, **7**, 1059
21 Sweet, G. E. and Bell, J. P. *J. Polym. Sci. (A-2)* 1972, **10**, 1273
22 Valenti, B., Bianchi, E., Greppi, G., Tealdi, A. and Ciferri, A. *J. Phys. Chem.* 1973, **77**, 389
23 Ceccorulli, G., Manescalchi, F., and Pizzoli, M. *Makromol. Chem.* 1975, **176**, 1163
24 Todoki, M. and Kawaguchi, T. *J. Polym. Sci. (Polym. Phys. Edn)* 1977, **15**, 1067
25 Cornibert, J., Marchessault, R. H., Allegrezza Jr, A. E. and Lenz, R. W. *Macromolecules* 1973, **6**, 676
26 Manzini, G., Crescenzi, V., Ciana, A., Ciceri, L., Della Fortuna, A. and Zotteri, L. *Europ. Polym. J.* 1973, **9**, 941
27 Prud'homme, R. E. and Marchessault, R. H. *Makromol. Chem.* 1974, **175**, 2705
28 Hobbs, S. Y. and Pratt, C. F. *Polymer* 1975, **16**, 462
29 Edwards, B. C. *J. Polym. Sci. (Polym. Phys. Edn)* 1975, **13**, 1387
30 Hughes, M. A. and Sheldon, R. P. *J. Appl. Polym. Sci.* 1964, **8**, 1541
31 Roberts, R. C. *Polymer* 1969, **10**, 117
32 Roberts, R. C. *J. Polym. Sci. (B)* 1970, **8**, 381
33 Nealy, D. L., Davis, T. G. and Kibler, C. J. *J. Polym. Sci. (A-2)* 1970, **8**, 2141
34 Holdsworth, P. J. and Turner-Jones, A. *Polymer* 1971, **12**, 195
35 Miller, G. W. *Thermochim. Acta* 1974, **8**, 129
36 Coppola, G., Fabbri, P., Pallesi, B., Alfonso, G. C., Dondero, G. and Pedemonte, E. *Makromol. Chem.* 1975, **176**, 767
37 Berndt, H. J., and Bossman, A. *Polymer* 1976, **17**, 241
38 Oswald, H. J., Turi, E. A., Harget, P. J. and Khanna, Y. P. *J. Macromol. Sci.* (Phys.), 1977, **3**, 231
39 Zachmann, H. G. and Schmidt, G. F. *Makromol. Chem.* 1962, **52**, 23
40 Yeh, G. S. Y. and Geil, P. H. *J. Macromol. Sci. (Phys.)* 1967, **1**, 235
41 Fakirow, S., Fisher, E. W., Hoffmann, R. and Schmidt, G. F. *Polymer* 1977, **18**, 1121
42 Miyagi, A., and Wunderlich, B. *J. Polym. Sci. (Polym. Phys. Edn)* 1972, **10**, 1401
43 Miyagi, A., and Wunderlich, B. *J. Polym. Sci. (Polym. Phys. Edn)* 1972, **10**, 2085
44 Tung, L. H. and Taylor, W. C. *J. Polym. Sci.* 1956, **21**, 144
45 Ziabicki, A. and Wasiak, A. *Kolloid. Z. Z. Polym.* 1967, **215**, 158
46 Alexander, L. E. 'X-Ray Diffraction Methods in Polymer Science', Wiley, New York, 1969
47 Ziabicki. A. 'Fundamentals of Fibre Formation' Wiley, London, 1976
48 Garrett, T. B. and Goldfarb, L. *J. Appl. Polym. Sci.* 1977, **21**, 1395
49 Peterlin, A. *J. Appl Phys.* 1964, **35**, 75
50 Warner, F. P., Brown, D. S. and Wetton, R. E. *J. Chem. Soc. (Faraday Trans. 1)* 1976, **72**, 1064
51 Kavesh, S. and Schulz J. M. *J. Polym. Sci. (A-2)* 1971, **9**, 85
52 Zachmann, H. G. and Stuart H. A. *Makromol. Chem.* 1960, **41**, 131
53 Zachmann, H. G. and Stuart, H. A. *Makromol. Chem.* 1960, **41**, 148
54 Hartley, F. D., Lord F. W. and Morgan, L. B. *Phil. Trans. Roy. Soc. (London)* 1954, **247**, 23
55 Weeks, J. J. *J. Res. Nat. Bur. Stand (A)* 1963, **67**, 441
56 Bell, J. P., Slade, P. E. and Dumbleton, J. H. *J. Polym. Sci. (A-2)* 1968, **6**, 1773
57 Fischer, E. W. and Fakirow, S. *J. Mater. Sci.* 1976, **11**, 1041
58 Hosemann, R. *Polymer* 1962, **3**, 349
59 Geil, P. H. *Ind. Eng Chem. (Prod. Res. Dev.)* 1975, **14**, 59
60 Hoffman, J. D. *SPE Trans.* 1964, **4**, 315
61 Wundelich, B. 'Macromolecular Physics', Academic Press, New York, 1973, Vol 1
62 Ikeda, M. and Mitsuishi, Y. *High Polym. Jpn* 1967, **24**, 376
63 Peterlin, A. *J. Polym. Sci. (Polym. Lett. Edn)* 1963, **1**, 279
64 Peterlin, A. *Polymer* 1965, **6**, 25
65 Collier, J. R. and Baer, E. *J. Appl. Polym. Sci.* 1966, **10**, 1409
66 Sanchez, I. C., Colson, J. P. and Eby, R. K. *J. Appl Phys.* 1973, **44**, 4332
67 Sanchez, I. C., Peterlin, A., Eby, R. K. and McCrackin, F. L. *J. Appl. Phys.* 1974, **45**, 4216
68 Overton, J. R. and Haynes, S. K. *J. Polym. Sci. (Polym. Symp.)* 1973, **43**, 9
69 Wlochowicz, A. and Przygocki, W. *J. Appl. Polym. Sci.* 1973, **17**, 1197
70 Karr, P. H., Pedrecki, P., Hendricks, R. W. and Lin, J. S. *Polym. Prepr.* 1978, **19**, 572
71 Van Krevelen, D. W. 'Properties of Polymers', Elsevier, Amsterdam, 1976